Heterogeneous & Homogeneous & Bio- & Nano-
CHEMCATCHEM
CATALYSIS

Accepted Article

Title: Phosphane-decorated Platinum Nanoparticles as Efficient Catalysts for H2 Generation from Ammonia Borane and Methanol

Authors: Patricia Lara Muñoz, Karine Philippot, and Andrés Suárez

To be cited as: *ChemCatChem* 10.1002/cctc.201801702

Link to VoR: http://dx.doi.org/10.1002/cctc.201801702

A Journal of
ChemPubSoc Europe

WILEY-VCH

www.chemcatchem.org

10.1002/cctc.201801702

WILEY-VCH

FULL PAPER

Phosphane-decorated Platinum Nanoparticles as Efficient Catalysts for H_2 Generation from Ammonia Borane and Methanol

Patricia Lara,*[a] Karine Philippot[b],[c] and Andrés Suárez[a]

Dedicated to Prof. Ernesto Carmona on occasion of his 70th birthday

Abstract: A series of narrowly dispersed Pt nanoparticles of 1.5-2.2 nm in size stabilized by bulky terphenylphosphane ligands has been synthesized by the organometallic method using $[Pt(dba)_2]$ as platinum source. These nanoparticles are highly efficient catalysts for hydrogen generation by methanolysis of ammonia borane ($H_3N{\cdot}BH_3$), providing notable TOF values of up to 284 min^{-1} at 30 °C and low catalyst loadings (0.14-0.19 mol%). Furthermore, catalysts separation (after distillation of the H_2-depleted ammonium tetramethoxyborate ($NH_4B(OMe)_4$) and methanol) and recycling were proven to be feasible, although an erosion of the catalytic activity was observed after three catalytic runs. These Pt nanoparticles have also been used as catalysts for tandem dehydrogenation of ammonia borane and hydrogenation of N-heterocycles, providing the reduction products of quinoline, phenanthridine, 2-methylquinoxaline and acridine in >90% yields under mild reaction conditions.

Introduction

Chemical energy release from the hydrogen molecule is considered as a practical alternative to replace fossil fuels, and the implementation of a global economy based on hydrogen as an energy vector ("Hydrogen Economy") has been envisaged.[1] At this regard, H_2-storage in a chemical reagent by formation of covalent bonds has attracted considerable attention.[2] Among the different possibilities explored,[3] the use of ammonia borane ($H_3N{\cdot}BH_3$) is particularly appealing for the controlled storage and supply of H_2 due to its high hydrogen gravimetric content (19.6 %wt) and favorable physical properties including high thermal stability, non-flammability and low toxicity.[4] Hydrogen generation from $H_3N{\cdot}BH_3$ can be accomplished by different methods,[3,5] including thermal and catalytic decomposition.[6] These methods present disadvantages such as the uncomplete release of the maximum available H_2 content (3 equiv) and formation of different by-products from which it is difficult to regenerate the $H_3N{\cdot}BH_3$ molecule.[7] As another method, solvolysis of $H_3N{\cdot}BH_3$ by a protic solvent such as water[8,9] or an alcohol[9] usually allow the release of the maximum H_2 content and the concomitant formation of a sole H_2-depleted by-product. Hydrogen generation from ammonia borane using methanol is particularly interesting given the high solubility of $H_3N{\cdot}BH_3$ in this solvent (23 %wt at 23 °C) and the long-term stability of the solutions. Moreover, methanolysis of $H_3N{\cdot}BH_3$ yields ammonium tetramethoxyborate ($NH_4B(OMe)_4$), which unlike the product formed by the hydrolysis of ammonia borane (ammonium metaborate, NH_4BO_2), can be easily reconverted to $H_3N{\cdot}BH_3$ by reaction with $LiAlH_4$ and NH_4Cl.[9]

Metal nanoparticles (NPs) are appealing catalytic systems due to their high proportion of surface atoms providing numerous active sites.[10] The design of well-controlled nanoparticles in terms of size, dispersion and surface state is crucial to achieve good levels of activity and selectivity in a catalytic process. In this context, the organometallic approach for the synthesis of metal nanoparticles has proven to be a powerful method to obtain small and well-controlled nanoparticles displaying hydrides and coordinated ligands at their surface.[11] Transition metal nanoparticles have been shown to catalyze $H_3N{\cdot}BH_3$ decomposition,[12] including the methanolysis of ammonia borane.[13] Most of the described systems of NPs are stabilized using porous materials such as oxide supports and resins that increase the weight of the resulting H_2-storage/delivery system.

Herein, we report the organometallic synthesis of Pt NPs stabilized by sterically demanding phosphanes containing terphenyl groups, and their use as catalysts in H_2 generation from ammonia borane and methanol.[14] A proper adjustment of the phosphane ligand and the phosphane/Pt ratio allowed to obtain small nanoparticles of 1.5-2.2 nm in size that display high catalytic activities. Furthermore, the feasibility of tandem $H_3N{\cdot}BH_3$ dehydrogenation and N-heterocycle hydrogenations catalyzed by these catalysts is demonstrated.

Results and Discussion

Synthesis and characterization of Pt·L nanoparticles

A series of platinum nanoparticles were easily synthesized by decomposing a THF solution of bis(dibenzylideneacetone)platinum, $[Pt(dba)_2]$, at room temperature under 3 bar of H_2 and in the presence of a phosphane containing a sterically demanding terphenyl group as stabilizing ligand. Three different phosphanes were tested: dimethyl-2,6-bis(2´,6´-dimethylphenyl)phenylphosphane, **L1**; diethyl-2,6-bis(2´,6´-dimethylphenyl)phenylphosphane, **L2**; and dimethyl-2,6-bis(2´,6´-di(isopropyl)phenyl)phenylphosphane, **L3** (Figure 1, Table 1). A color change from violet to dark brown was

[a] Dr. P. Lara, Dr. A. Suárez
Instituto de Investigaciones Químicas (IIQ), Departamento de Química Inorgánica and Centro de Innovación en Química Avanzada (ORFEO-CINQA). Consejo Superior de Investigaciones Científicas (CSIC) and Universidad de Sevilla. Avda. Américo Vespucio, 49, 41092 Sevilla (Spain)
E-mail: patricia@iiq.csic.es
[b] Dr. K. Philippot
CNRS, LCC (Laboratoire de Chimie de Coordination). 205, Route de Narbonne, BP 44099, F-31077 Toulouse Cedex 4, France
[c] Dr. K. Philippot
Université de Toulouse, UPS, INPT, F-31077 Toulouse Cedex 4, France

observed after 3 h of reaction, but the reaction mixture was kept under vigorous stirring for 14 h to ensure the total decomposition of the precursor. Then, the dihydrogen pressure was released, and the NPs were isolated by precipitation with cold pentane, giving rise to black powders that were further used for catalytic studies. In order to obtain the best conditions in terms of dispersion and homogeneity, different ligand to metal ratios (**L**/Pt = 0.2 or 0.5) were examined. The metal content of the purified nanoparticles was obtained by Inductive Coupled Plasma (ICP) with values of 52-69%wt Pt (Table 1). The morphology and size of the nanoparticles were determined by TEM (transmission electron microscopy). Mean sizes in the range 1.5-2.2 nm depending on the ligand used were measured (Table 1, Figure 2).

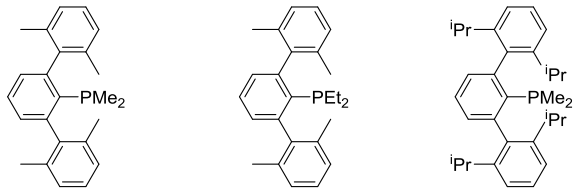

L1 **L2** **L3**

Figure 1. Terphenylphosphanes **L** used to stabilize Pt nanoparticles.

The first Pt/phosphane sample (Pt·**L1**$^{0.2}$) was prepared employing 0.2 molar equiv of ligand **L1** as stabilizer with respect to platinum. In these synthesis conditions, nanoparticles of 2.2 (0.5) nm were formed (Figure 2). When the reaction was performed using 0.5 equiv of ligand **L1**, nanoparticles Pt·**L1**$^{0.5}$ displaying a better dispersion and presenting a slightly smaller size (2.0 (0.3) nm) were obtained (Figure 2). This trend (smaller size with more ligand at the surface) has already been observed for Ru and Pt NPs stabilized with different ligands.[15,16] The third Pt/phosphane sample (Pt·**L2**$^{0.2}$) was synthesized with 0.2 equiv of ligand **L2**, leading to a homogeneous population of NPs having a mean size of 1.5 (0.2) nm. Finally, a fourth colloid was prepared in the presence of 0.2 equiv of ligand **L3** (Pt·**L3**$^{0.2}$). In this case, nanoparticles of mean size 2.0 (0.5) nm were observed by TEM.

Table 1. Terphenylphosphane stabilized Pt NPs.

Pt NPs	**L**/Pt ratio	%wt Pt[a]	Mean size [nm][b]
Pt·**L1**$^{0.2}$	0.2	64	2.2 (0.5)
Pt·**L1**$^{0.5}$	0.5	52	2.0 (0.3)
Pt·**L2**$^{0.2}$	0.2	67	1.5 (0.2)
Pt·**L3**$^{0.2}$	0.2	69	2.0 (0.5)

[a] %wt Pt content as determined by ICP. [b] Measured from TEM images. Standard deviations in parentheses.

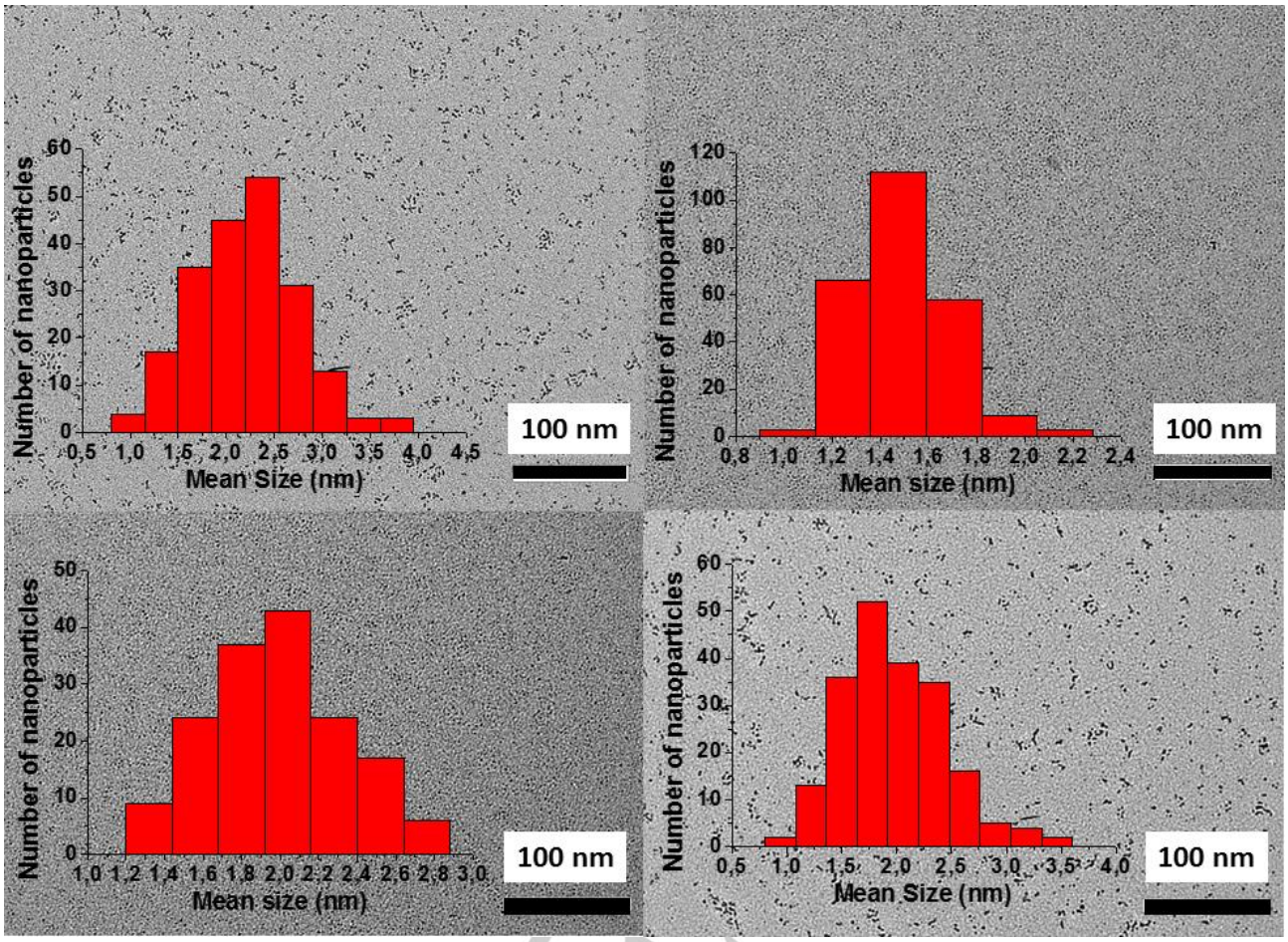

Figure 2. TEM images and size histograms of Pt·**L1**$^{0.2}$ (top, left) , Pt·**L1**$^{0.5}$ (bottom, left), Pt·**L2**$^{0.2}$ (top, right) and Pt·**L3**$^{0.2}$ (bottom, right).

High-resolution transmission electron microscopy (HRTEM) analysis performed on THF colloidal solution of Pt·**L1**$^{0.2}$ showed the high crystalline character of the nanoparticles and their face-centered cubic structure. Fast Fourier transformation (FFT) evidenced reflections that correspond to the (002), (220) and (204) atomic planes.

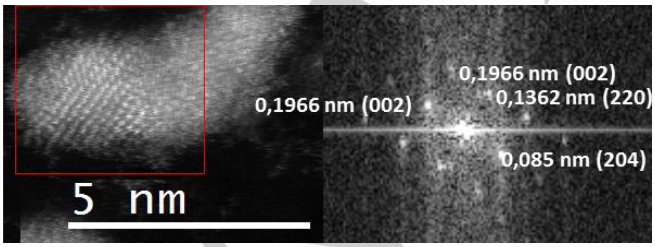

Figure 3. HRTEM (left) and FFT (right) images obtained for Pt·**L1**$^{0.2}$.

The composition of the particles was confirmed by High angle annular dark field imaging (HAADF) coupled with energy-dispersive X-ray spectrometry (EDX) mapping using scanning transmission electron microscopy (STEM). The EDX spectrum recorded in a selected area of the grid revealed some peaks that can be attributed to Pt (at ca. 1.6, 2.1, 2.8, 8.2 and 9.4 keV) despite an overlapping with peak for phosphorous at ca. 2.0 keV. (see SI).

H_2 generation by methanolysis of ammonia borane

The catalytic activity of the terphenylphosphane stabilized platinum nanoparticles Pt·**L** was evaluated in the generation of H_2 from methanol solutions of $H_3N{\cdot}BH_3$. Reactions were performed at 30 °C using 0.14-0.19 mol% Pt loadings of Pt·**L** NPs (Figure 4, Table 2). The monitoring of the catalytic performance was done by measuring the increase of the pressure of gas evolved. Using Pt·**L1**$^{0.2}$ as catalyst, the reaction started with no induction period and led to complete conversion in less than 8 min with the evolution of 3 mol H_2 per mol of $H_3N{\cdot}BH_3$. A significant turnover

frequency (TOF; calculated from mmol of H_2/(mmol Pt x time)) of 191 min^{-1} was found (Table 2, entry 1). ^{11}B NMR spectroscopy analysis of the hydrogen depleted solution showed the presence of only a singlet at δ 7.5 ppm, supporting the quantitative formation of ammonium tetramethoxyborate, $NH_4B(OMe)_4$ (Figure S2).[9] The NPs synthesized with a **L1**/Pt ratio of 0.5 appeared significantly less active than their Pt·**L1**$^{0.2}$ counterparts (entries 1 and 2) showing a TOF value of 107 min^{-1} against 191 min^{-1}, respectively. This decrease of activity can be attributed to a higher coverage of the nanoparticle metal surface by the phosphane ligands that prevents substrates from accessing the reactive sites, as previously observed in other catalytic processes mediated by ligand-stabilized NPs.[16] Hence, the catalytic behavior of the terphenylphosphane stabilized Pt nanoparticles with **L**/metal ratios of 0.2 was compared, showing that the steric properties of the phosphane ligand have a marked influence on the catalytic activity. Nanoparticles Pt·**L2**$^{0.2}$, which differ from Pt·**L1**$^{0.2}$ in the alkyl substituent of the phosphane ligand (methyl and ethyl groups, respectively), were found to be a slower catalyst (entry 3). Alternatively, nanoparticles based on **L3**, having a more sterically demanding terphenyl group, provided a ca. 1.5-fold increase of the catalytic activity with respect to Pt·**L1**$^{0.2}$, giving rise to a notable TOF of 284 min^{-1} (entry 4). This high catalytic performance compares favorably with activities provided by other metal catalysts in the methanolysis of $H_3N{\cdot}BH_3$ (see SI, Table S1). It is also worth mentioning that with Pt·**L3**$^{0.2}$, the catalyst loading could be further decreased to 0.08 mol% without a significant impact on the catalytic activity (entry 5; Figure S3). Furthermore, TEM analysis of the colloid Pt·**L3**$^{0.2}$ after the catalytic reaction showed a very slight increase in the nanoparticles size to 2.3 (0.4) nm (Figure S4).

In order to obtain a better insight of the potential of our catalytic system, a solution of 15.2 mmol of $H_3N{\cdot}BH_3$ in MeOH was added to a colloidal suspension of 2.5 μmol Pt·**L3**$^{0.2}$ (0.016 mol% Pt) in MeOH at 25 °C, and the volume of gas evolved was measured in a gas burette (Figure 5). A steady H_2 production was observed until approximately 90% conversion of $H_3N{\cdot}BH_3$, with an average TOF of 122 min^{-1}. Overall 18240 mmol H_2 per mmol Pt were produced in the reaction.

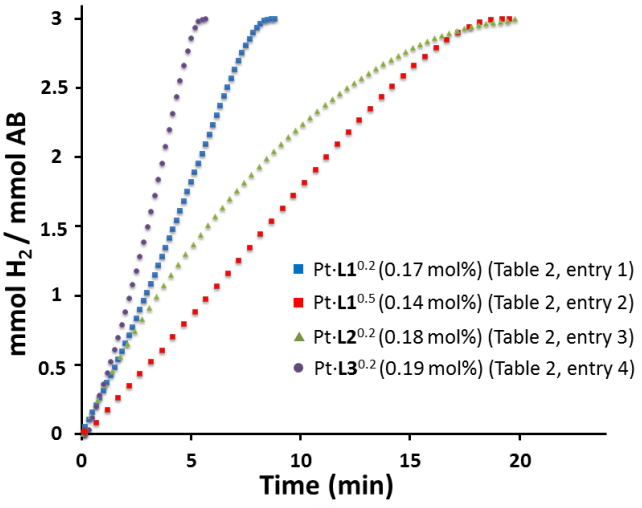

Figure 4. Hydrogen evolution from the methanolysis of $H_3N{\cdot}BH_3$ catalyzed by Pt·**L** nanoparticles. See Table 2 for experimental details.

Table 2. Methanolysis of $H_3N{\cdot}BH_3$ catalyzed by Pt·**L** NPs.[a]

Entry	Pt·**L**	Cat. loading[b] [mol%]	Conv. [%] (time, [min])	TOF [min^{-1}]
1	Pt·**L1**$^{0.2}$	0.17	100 (8)	191
2	Pt·**L1**$^{0.5}$	0.14	100 (19)	107
3	Pt·**L2**$^{0.2}$	0.18	100 (19)	87
4	Pt·**L3**$^{0.2}$	0.19	100 (5.5)	284
5[b]	Pt·**L3**$^{0.2}$	0.08	100 (15)	253

[a] Reactions conditions, unless otherwise noted: 30 °C, [$H_3N{\cdot}BH_3$] = 1.2 M. TOF values as calculated from (mmol of H_2/mmol Pt) x min^{-1}. [b] [$H_3N{\cdot}BH_3$] = 1.7 M.

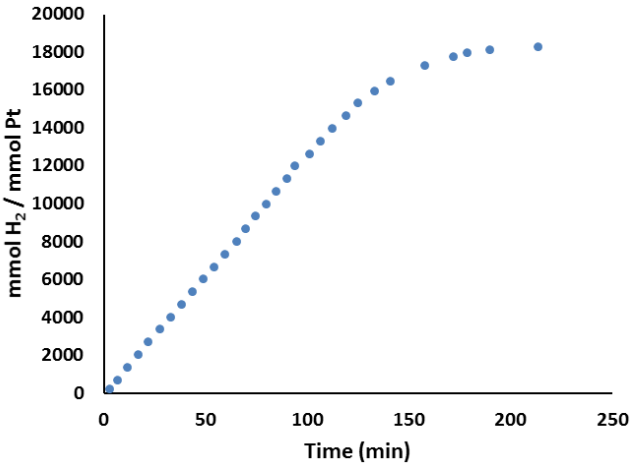

Figure 5. Large scale methanolysis of $H_3N{\cdot}BH_3$ catalyzed by Pt·**L3**$^{0.2}$ nanoparticles. Reactions conditions: 0.016 mol% Pt, 25 °C, [$H_3N{\cdot}BH_3$] = 1.8 M.

Ammonium tetramethoxyborate ($NH_4B(OMe)_4$) can be easily sublimated under reduced pressure, and its reconversion to $H_3N{\cdot}BH_3$ has been demonstrated.[9] Since clean transformation of $H_3N{\cdot}BH_3$ to ammonium tetramethoxyborate was observed in the methanolysis of $H_3N{\cdot}BH_3$ catalyzed by the Pt·**L** nanoparticles (see ^{11}B NMR spectroscopy analysis), a reusable H_2 delivery system based on catalyst reutilization after vacuum distillation removal of the H_2-depleted by-product and MeOH was tested (Figure 6). Over three reuse cycles, complete conversion of $H_3N{\cdot}BH_3$ was observed in the reactions mediated with Pt·**L1**$^{0.2}$, Pt·**L2**$^{0.2}$ and

Pt·**L3**$^{0.2}$ nanoparticles, retaining the catalysts 55-66% of their initial activities after the third reutilization.

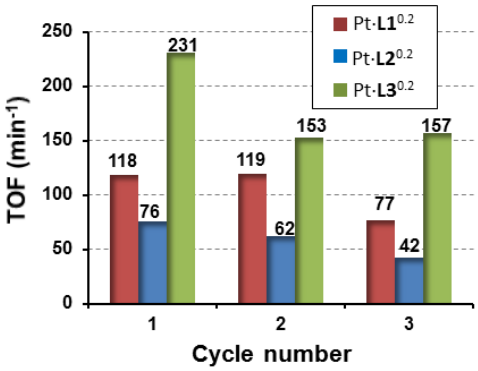

Figure 6. Recycling experiments of Pt·**L** nanoparticles. Reaction conditions: 0.2 mol% Pt, 25 °C, MeOH, [$H_3N{\cdot}BH_3$] = 1.3 M. TOF values as calculated from (mmol of H_2/mmol Pt) x min^{-1}.

Tandem $H_3N{\cdot}BH_3$ dehydrogenation/N-heterocycle hydrogenation

In addition to its use as energy carrier, ammonia borane has found applications as a reductant in synthetic organic chemistry,[4e,17] and the development of metal-catalyzed reductions using $H_3N{\cdot}BH_3$ as hydrogen source has been explored.[18] Interestingly, hydrogen generation by ammonia borane methanolysis allows for an easy separation of the reaction products from the dehydrogenated by-products. Therefore, tandem $H_3N{\cdot}BH_3$ dehydrogenation/hydrogenation of N-heterocycles catalyzed by Pt·**L** nanoparticles was examined to probe the potential of the catalysts in such a tandem process (Table 3). Hydrogenation of quinoline was cleanly carried out with 3 equivalents of $H_3N{\cdot}BH_3$ in 91 and 58% yields using 1.0 mol% of Pt·**L1**$^{0.2}$ and Pt·**L3**$^{0.2}$, respectively (entries 1 and 2). Moreover, nanoparticles Pt·**L1**$^{0.2}$ were also effective in the reduction of other N-heterocycles such as phenanthridine, 2-methylquinoxaline and acridine providing the corresponding reduction products in >90% yield (entries 3-5).

Conclusions

Narrowly dispersed Pt nanoparticles stabilized with sterically demanding terphenylphosphane ligands have been synthesized. These nanoparticles displayed high activities in the generation of H_2 by methanolysis of $H_3N{\cdot}BH_3$. Thus, by a simple adjustment of the structure of the phosphane ligand and the phosphane/Pt ratio, high turnover frequencies of up to 283 min^{-1} were observed at 30 °C and low catalyst loadings. Also, reusability studies of the catalysts have shown it is feasible although an erosion of the catalytic activity was observed after three catalytic runs. Finally, the possibility to use these catalysts for tandem $H_3N{\cdot}BH_3$ dehydrogenation/N-heterocycle hydrogenation reactions has been demonstrated. It is worth mentioning that with the colloidal catalysts here described, additional weight and effects produced by supports as used with other nanocatalysts for the target reaction are avoided.

Table 3. Tandem $H_3N{\cdot}BH_3$ methanolysis/*N*-heterocycle hydrogenation with Pt·**L** nanoparticles.[a]

Entry	Pt·**L**	Substrate	Product	yield [%]
1	Pt·**L1**$^{0.2}$	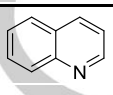	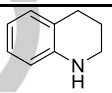	91
2	Pt·**L3**$^{0.2}$			58
3	Pt·**L1**$^{0.2}$	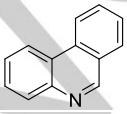	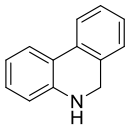	92
4	Pt·**L1**$^{0.2}$	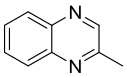	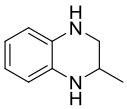	>99
5	Pt·**L1**$^{0.2}$	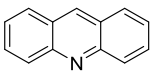	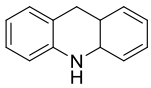	91

[a] Reaction conditions: 3 equiv $H_3N{\cdot}BH_3$, 1.0 mol% Pt, 60 °C, MeOH, [S] = 0.3 M, 21 h.

Experimental Section

General procedures and characterization techniques. All the reactions have been carried out in a glovebox or under nitrogen or argon atmosphere using Schlenk-type techniques. Solvents have been dried by already known procedures and distilled under argon or nitrogen atmosphere before their use. Methanol was dried with sodium methoxide (NaOMe) and distilled under argon. Ammonia borane was purchased from Aldrich, and used without any further purification. Terphenylphosphane ligands **L1**,[19] **L2**[19] and **L3**[20] were prepared according to already published procedures. [$Pt(dba)_2$] was obtained by a previously reported method,[21] and its %wt of Pt was determined by ICP. Pt NPs were analyzed by TEM and HRTEM after deposition of a drop of the crude THF colloidal solution or a drop of a solution of the isolated nanoparticles after dispersion in THF on a covered holey copper grid, respectively. TEM analyses were performed at the Centro de Investigación, Tecnología e Innovación (CITIUS) of the University of Sevilla by using a Philips CM-200 working at 200 kV with a point resolution of 2.8 Å. The approximation of the particles mean size was made through a manual analysis of enlarged micrographs by measuring ca. 300 particles on a given grid. HRTEM observations were carried out at the TEMSCAN-UPS with a JEOL JEM 2010 - EDS electron microscope working at 200 kV with a resolution point of 2.35 Å and equipped with a EDX analyzer (Noran). FFT treatments have been carried out with Digital Micrograph Version 1.80.70. ICP analyses were performed at the "Mikroanalytisches Labor Pascher". ^{11}B NMR spectra were obtained on a

Bruker DPX-300 spectrometer, and ^{11}B shifts were referenced to external $BF_3{\cdot}OEt_2$.

Nanoparticles synthesis. [$Pt(dba)_2$] (0.250 g, 0.36 mmol) was introduced in a Fisher-Porter vessel and dissolved in 35 mL of freshly distilled and degassed THF by argon bubbling. The resulting violet solution was cooled to -60 ºC and a solution of 15 mL of THF containing ligand **L** (0.074 mmol for nanoparticles **Pt·L1**$^{0.2}$, **Pt·L2**$^{0.2}$ and **Pt·L3**$^{0.2}$; and 0.19 mmol for nanoparticles **Pt·L1**$^{0.5}$) was added into the reactor. The Fisher-Porter bottle was pressurized with 3 bar of H_2 and the solution was left to reach slowly the room temperature under vigorous stirring. The homogenous solution, which turns black after 30 minutes of reaction, was kept under stirring overnight at room temperature. After this period of time, excess of H_2 was eliminated and the volume of solvent was reduced to 10 mL under vacuum. Pentane (40 mL) was added to the colloidal suspension which was cooled down to -30 ºC to precipitate the particles. After filtration under argon with a cannula, the black solid powder was washed twice with pentane (2 x 40 mL) and dried under vacuum. For Pt content determination by ICP and TEM analysis of the nanoparticles, see Table 1.

Catalytic reactions

Experimental setup for small scale H_2 production. H_2 generation was followed up using a Fisher-Porter vessel (25 mL) connected to a vacuum line and coupled to a ESI pressure gauge model GS4200-USB (0-6 bar) plugged to a computer.

Representative procedure for hydrogen generation. A freshly prepared solution of ammonia borane (1.9 M) in MeOH (1.0 mL, 1.9 mmol $H_3N{\cdot}BH_3$) was added to a colloidal suspension of the nanoparticles Pt·**L1**$^{0.2}$ (1.0 mg, 3.3 μmol Pt) in MeOH (0.5 mL) thermostated to 30 ºC and stirred at 750 rpm. H_2 generation was monitored by registering the increase of pressure in the system. Quantitative formation of ammonium tetramethoxyborate ($NH_4B(OMe)_4$) was determined by ^{11}B NMR spectroscopy.

Large scale hydrogen generation. A freshly prepared solution of ammonia borane (1.9 M) in MeOH (8.0 mL, 15.2 mmol $H_3N{\cdot}BH_3$) was added over 16 min to a colloidal suspension of nanoparticles Pt·**L3**$^{0.2}$ (0.7 mg, 2.5 μmol Pt) in MeOH (0.25 mL) thermostated to 25 ºC and stirred at 750 rpm. H_2 generation was monitored by measuring the gas evolved in a gas burette. Quantitative formation of ammonium tetramethoxyborate was determined by ^{11}B NMR spectroscopy.

Representative procedure for H_2 generation with catalyst recycling. A solution of ammonia borane (1.9 M) in MeOH (1.0 mL, 1.9 mmol $H_3N{\cdot}BH_3$) was added to a colloidal suspension of the nanoparticles Pt·**L1**$^{0.2}$ (1.0 mg, 3.3 μmol Pt) in MeOH (0.5 mL) thermostated to 25 ºC and stirred at 750 rpm. H_2 generation was monitored by registering the increase of pressure in the system. After the reaction proceeded to completion, solvent and ammonium tetramethoxyborate were distilled off under vacuum. MeOH (0.5 mL) and a solution 1.9 M of $H_3N{\cdot}BH_3$ in MeOH (1.0 mL, 1.9 mmol) were successively added to the nanoparticles and H_2 generation was again monitored. The process was repeated over three times.

General procedure for tandem $H_3N{\cdot}BH_3$ methanolysis/N-heterocycle hydrogenation. A 10 mL Fisher-Porter vessel was charged with a suspension of Pt·**L1**$^{0.2}$ (1.0 mg, 3.8 μmol Pt) and the corresponding N-heterocycle (0.38 mmol) in MeOH (0.5 mL), and 0.75 mL (1.1 mmol of $H_3N{\cdot}BH_3$) of a freshly prepared solution of $H_3N{\cdot}BH_3$ in MeOH was added. The reaction mixture was heated to 60 ºC for 21 h. CAUTION: hydrogen pressure is developed. Product yield was determined by ^1H NMR spectroscopy using mesitylene as an internal standard.

Acknowledgements

Financial support (FEDER contribution) from the Spanish MINECO (CTQ2016-80814-R and CTQ2016-81797-REDC) is gratefully acknowledged. CNRS and Université Fédérale de Toulouse are also acknowledged for financial supports. Prof. Ernesto Carmona is thanked for a generous loan of terphenylphosphane ligands. V Collière is thanked for HRTEM - EDX measurements.

Keywords: nanoparticles • platinum • phosphane ligands • dehydrogenation • ammonia borane

[1] a) *Hydrogen as a Future Energy Carrier*, Eds. A. Zuttel, A. Borgschulte, L. Schlapbach, **2008**, Wiley-VCH; b) N. Armaroli, V. Balzani, *ChemSusChem* **2011**, *4*, 21−26.

[2] U. Eberle, M. Felderhoff, F. Schüth, *Angew. Chem. Int. Ed.* **2009**, *48*, 6608−6630.

[3] M. Yadav, Q. Xu, *Energy Environ. Sci.* **2012**, *5*, 9698−9725.

[4] a) T. B. Marder, *Angew. Chem. Int. Ed.* **2007**, *46*, 8116−8118; b) B. Peng, J. Chen, *Energy Environ. Sci.* **2008**, *1*, 479−483; c) U. B. Demirci, *Int. J. Hydrogen Energy* **2017**, *42*, 9978−10013; d) C. W. Hamilton, R. T. Baker, A. Staubitz, I. Manners, *Chem. Soc. Rev.* **2009**, *38*, 279−293; e) Z. Huang, T. Autrey, *Energy Environ. Sci.* **2012**, *5*, 9257−9268; f) Q-L. Zhu, Q. Xu, *Energy Environ. Sci.* **2015**, *8*, 478−512; g) G. Moussa, R. Moury, U. B. Demirci, T. Şener, P. Miele, *Int. J. Energy Res.* **2013**, *37*, 825−842.

[5] A. Staubitz, A. P. M. Robertson, I. Manners, *Chem. Rev.* **2010**, *110*, 4079−4124.

[6] a) S. Bhunya, T. Malakar, G. Ganguly, A. Paul, *ACS Catal.* **2016**, *6*, 7907−7934; b) A. Rossin, M. Peruzzini, *Chem. Rev.* **2016**, *116*, 8848−8872.

[7] N. C. Smythe, J. C. Gordon, *Eur. J. Inorg. Chem.* **2010**, 509−521.

[8] a) U. Sanyal, U. B. Demirci, B. R. Jagirdar, P. Miele, *ChemSusChem* **2011**, *4*, 1731−1739; b) H-L. Jiang, Q. Xu, *Catal. Today* **2011**, *170*, 56−63; c) M. Zahmakiran, S. Özkar, *Top. Catal.* **2013**, *56*, 1171−1183; d) F. Fu, C. Wang, A. M. Martínez-Villacorta, A. Escobar, H. Chong, X. Wang, S. Moya, L. Salmon, E. Fouquet, J. Ruiz, D. Astruc, *J. Am. Chem. Soc.* **2018**, *140*, 10034-10042; e) S. Akbayrak, S. Özkar, *Int. J. Hydrogen Energy* **2018**, *43*, 18592−18606.

[9] P. V. Ramachandran, P. D. Gagare, *Inorg. Chem.* **2007**, *46*, 7810−7817.

[10] a) *Nanotechnology in Catalysis*, *Vol. 3* (Eds.: B. Zhou, S. Han, R. Raja, G. Somorjai), Kluwer Academic/Plenum Publisher, New York, **2003**; b) A. Roucoux, K. Philippot in *Handbook of Homogeneous Hydrogenations, Vol. 9* (Eds.: J. G. de Vries, C. J. Elsevier), Wiley-VCH, Weinheim, **2007**, pp. 217–255; c) *Nanoparticles and Catalysis* (Ed.: D. Astruc), Wiley-VCH, Weinheim, **2008**.

[11] K. Philippot, B. Chaudret in *Comprehensive Organometallic Chemistry III* (Eds: R. H. Crabtree, M. P. Mingos), Elsevier, Volume 12–Applications III: Functional Materials, Environmental and Biological Applications, (Volume Ed: D. O'Hare), **2007**, Chap. 12–03, pp. 71–99.

[12] a) Y. Zhu, N. S. Hosmane, *Coord. Chem. Rev.* **2015**, *293–294*, 357–367; b) W-W. Zhan, Q-L. Zhu, Q. Xu, *ACS Catal.* **2016**, *6*, 6892−6905; c) M. Zahmakiran, S. Özkar, *Top. Catal.* **2013**, *56*, 1171-1183.

[13] a) D. Özhava, S. Özkar, *Appl. Catal. B: Environ.* **2016**, *181*, 716-726; b) D. Özhava, S. Özkar, *Int. J. Hydrogen Energy* **2015**, *40*, 10491-10501; c) S. Çalışkan, M. Zahmakıran, S. Özkar, *Appl. Catal. B: Environ.* **2010**, *93*, 387-394; d) J-K. Sun, W-W. Zhan, T. Akita, Q. Xu, *J. Am. Chem. Soc.* **2015**, *137*, 7063-7066; e) D. Özhava, N. Z. Kiliçaslan, S. Özkar, *Appl. Catal., B: Environ.* **2015**, *162*, 573-582; f) H-B. Dai, X-D. Kang, P. Wang, *Int. J. Hydrogen Energy* **2010**, *35*, 10317-10323; g) S. Peng, J. Liu, J. Zhang, F. Wang, *Int. J. Hydrogen Energy* **2015**, *40*, 10856-10866; h) H. Erdoğan, Ö. Metin, S. Özkar, *Phys. Chem. Chem. Phys.* **2009**, *11*,

10519-10525; i) S. B. Kalidindi, U. Sanyal, B. R. Jagirdar, *Phys. Chem. Chem. Phys.* **2008**, *10*, 5870-5874; j) M. Yurderi, A. Bulut, I. E. Ertas, M. Zahmakiran, M. Kaya, *Appl. Catal., B: Environ.* **2015**, *165*, 169-175; k) D. Sun, V. Mazumder, Ö. Metin, S. Sun, *ACS Catal.* **2012**, *2*, 1290-1295; l) P. Li, Z. Xiao, Z. Liu, J. Huang, Q. Li, D. Sun, *Nanotechnology* **2014**, *26*, 025401; m) D. Sun, P. Li, B. Yang, Y. Xu, J. Huang, Q. Li, *RSC Adv.* **2016**, *6*, 105940-105947; n) Y. Karataş, M. Gülcan, M. Çelebi, M. Zahmakiran, *ChemistrySelect* **2017**, *2*, 9628−9635; o) C. Yu, J. Fu, M. Muzzio, T. Shen, D. Su, J. Zhu, S. Sun, *Chem. Mater.* **2017**, *29*, 1413−1418; p) D. Özhava, S. Özkar, *Mol. Catal.* **2017**, *439*, 50−59; q) D. Özhava, S. Özkar, *Appl. Catal., B: Environ.* **2018**, *237*, 1012−1020; r) Y. Fang, J. Li, T. Togo, F. Jin, Z. Xiao, L. Liu, H. Drake, X. Lian, H.-C. Zhou, *Chem* **2018**, *4*, 555−563.

[14] For selected examples of Pt-based catalysts for ammonia borane dehydrogenation: a) F. Cheng, H. Ma, Y. Li, J. Chen, *Inorg. Chem.* **2007**, *46*, 788−794; b) X. Yang, F. Cheng, J. Liang, Z. Tao, J. Chen, *Int. J. Hydrogen Energy* **2009**, *34*, 8785−8791; c) X. Yang, F. Cheng, J. Liang, Z. Tao, J. Chen, *Int. J. Hydrogen Energy* **2011**, *36*, 1984−1990; d) X. Yang, F. Cheng, Z. Tao, J. Chen, *J. Power Sources* **2011**, *196*, 2785−2789; e) A. Aijaz, A. Karkamkar, Y. J. Choi, N. Tsumori, E. Rönnebro, T. Autrey, H. Shioyama, Q. Xu, *J. Am. Chem. Soc.* **2012**, *134*, 13926−13929; g) X. Wang, D. Liu, S. Song, H. Zhang, *Chem. Eur. J.* **2013**, *19*, 8082−8086; h) M. Rakap, *Appl. Catal., A: General* **2014**, *478*, 15−20; i) M. Li, J. Hu, Z. Chen, H. Lu, *RSC Adv.* **2014**, *4*, 41152−41158; j) J. Zhang, C. Chen, S. Chen, Q. Hu, Z. Gao, Y. Li, Y. Qin, *Catal. Sci. Technol.* **2017**, *7*, 322−329; k) T. Kamegawa, T. Nakaue, *Chem. Commun.* **2015**, *51*, 16802−16805; l) W. Chen, J. Ji, X. Duan, G. Qian, P. Li, X. Zhou, D. Chen, W. Yuan, *Chem. Commun.* **2014**, *50*, 2142−2144; m) R. P. Shrestha, H. V. K. Diyabalanage, T. A. Semelsberger, K. C. Ott, A. K. Burrell, *Int. J. Hydrogen Energy* **2009**, *34*, 2616−2621.

[15] a) P. Lara, O. Rivada-Wheelaghan, S. Conejero, R. Poteau, K. Philippot, B. Chaudret, *Angew. Chem.* **2011**, *123*, 12286−12290; *Angew. Chem. Int. Ed.* **2011**, *50*, 12080−12084; b) C. Pan, K. Pelzer, K. Philippot, B. Chaudret, F. Dassenoy, P. Lecante, M.-J. Casanove, *J. Am. Chem. Soc.* **2001**, *123*, 7584−7593.

[16] P. Lara, A. Suárez, V. Collière, K. Philippot, B. Chaudret, *ChemCatChem* **2014**, *6*, 87-90.

[17] a) L. Shi, Y. Liu, Q. Liu, B. Wei, G. Zhang, *Green Chem.* **2012**, *14*, 1372−1375; b) X. Yang, L. Zhao, T. Fox, Z.-X. Wang, H. Berke, *Angew. Chem. Int. Ed.* **2010**, *49*, 2058−2062; c) X. Yang, T. Fox, H. Berke, *Chem. Commun.* **2011**, *47*, 2053−2055; d) X. Yang, T. Fox, H. Berke, *Tetrahedron* **2011**, *67*, 7121−7127; e) P. V. Ramachandran, P. D. Gagare, K. Sakavuyi, P. Clark, *Tetrahedron Lett.* **2010**, *51*, 3167–3169.

[18] a) S. Fu, N-Y. Chen, X. Liu, Z. Shao, S-P. Luo, Q. Liu, *J. Am. Chem. Soc.* **2016**, *138*, 8588−8594; b) R. Barrios-Francisco, J. J. García, *Appl. Catal., A: General* **2010**, *385*, 108−113; c) E. Vasilikogiannaki, C. Gryparis, V. Kotzabasaki, I. N. Lykakis, M. Stratakis, *Adv. Synth. Catal.* **2013**, *355*, 907−911; d) E. Vasilikogiannaki, I. Titilas, G. Vassilikogiannakis, M. Stratakis, *Chem. Commun.* **2015**, *51*, 2384−2387; e) J. K. Pagano, J. P. W. Stelmach, R. Waterman, *Dalton Trans.* **2015**, *44*, 12074−12077; f) C. E. Hartmann, V. Jurčík, O. Songis, C. S. J. Cazin, *Chem. Commun.* **2013**, *49*, 1005−1007; g) X. Ma, Y-X. Zhou, H. Liu, Y. Li, H-L. Jiang, *Chem. Commun.* **2016**, *52*, 7719−7722; h) H. Göksu, S. F. Ho, Ö. Metin, K. Korkmaz, A. Mendoza Garcia, M. S. Gültekin, S. Sun, *ACS Catal.* **2014**, *4*, 1777−1782; i) B. Nişancı, K. Ganjehyan, Ö. Metin, A. Daştan, B. Török, *J. Mol. Catal., A: Chem.* **2015**, *409*, 191−197; j) M. A. Esteruelas, P. Nolis, M. Oliván, E. Oñate, A. Vallribera, A. Vélez, *Inorg. Chem.* **2016**, *55*, 7176−7181; k) A. Brzozowska, L. M. Azofra, V. Zubar, I. Atodiresei, L. Cavallo, M. Rueping, O. El-Sepelgy, *ACS Catal.* **2018**, *8*, 4103−4109; l) S. Byun, Y. Song, B. M. Kim, *ACS Appl. Mater. Interfaces* **2016**, *8*, 14637−14647; m) Ö. Metin, A. Mendoza-Garcia, D. Dalmızrak, M. S. Gültekin, S. Sun, *Catal. Sci. Technol.* **2016**, *6*, 6137-6143; n) P. Eghbali, B. Nişancı, Ö. Metin, *Pure Appl. Chem.* **2018**, *90*, 327-335.

[19] L. Ortega-Moreno, M. Fernández-Espada, J. J. Moreno, C. Navarro-Gilabert, J. Campos, S. Conejero, J. López-Serrano, C. Maya, R. Peloso, E. Carmona, *Polyhedron* **2016**, *116*, 170−181.

[20] L. Ortega-Moreno, R. Peloso, C. Maya, A. Suárez, E. Carmona, *Chem. Commun.* **2015**, *51*, 17008−17011.

[21] K. Moseley, P. M. Maitlis, *Chem. Commun.* **1971**, 982-983.

10.1002/cctc.201801702

WILEY-VCH

Entry for the Table of Contents (Please choose one layout)

Layout 1:

FULL PAPER

The synthesis of a series of narrowly dispersed Pt nanoparticles stabilized with sterically demanding terphenylphosphane ligands is reported. These nanoparticles are highly efficient catalysts for hydrogen generation by methanolysis of $H_3N{\cdot}BH_3$ (TOF up to 283 min^{-1}). Reusability studies of the catalysts have been carried out, as well as the use of these nanoparticles for tandem $H_3N{\cdot}BH_3$ dehydrogenation/N-heterocycle hydrogenation processes.

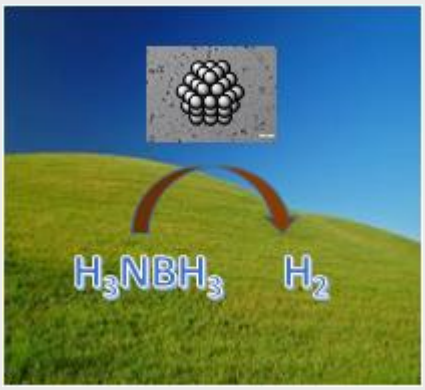

P. Lara, K. Philippot, A. Suárez*

Page No. – Page No.

Phosphane-decorated Platinum Nanoparticles as Efficient Catalysts for H_2 Generation from Ammonia Borane and Methanol